

Thermophysical Property Measurements of Salt Mixtures



**Approved for public release.
Distribution is unlimited.**

N. Dianne Bull Ezell
Ryan Gallagher
Nicholas Russell
Alex Martin
Abbey McAlister
Jake McMurray

August 2020

DOCUMENT AVAILABILITY

Reports produced after January 1, 1996, are generally available free via US Department of Energy (DOE) SciTech Connect.

Website: www.osti.gov/

Reports produced before January 1, 1996, may be purchased by members of the public from the following source:

National Technical Information Service
5285 Port Royal Road
Springfield, VA 22161
Telephone: 703-605-6000 (1-800-553-6847)
TDD: 703-487-4639
Fax: 703-605-6900
E-mail: info@ntis.gov
Website: <http://classic.ntis.gov/>

Reports are available to DOE employees, DOE contractors, Energy Technology Data Exchange representatives, and International Nuclear Information System representatives from the following source:

Office of Scientific and Technical Information
PO Box 62
Oak Ridge, TN 37831
Telephone: 865-576-8401
Fax: 865-576-5728
E-mail: report@osti.gov
Website: <http://www.osti.gov/contact.html>

This report was prepared as an account of work sponsored by an agency of the United States Government. Neither the United States Government nor any agency thereof, nor any of their employees, makes any warranty, express or implied, or assumes any legal liability or responsibility for the accuracy, completeness, or usefulness of any information, apparatus, product, or process disclosed, or represents that its use would not infringe privately owned rights. Reference herein to any specific commercial product, process, or service by trade name, trademark, manufacturer, or otherwise, does not necessarily constitute or imply its endorsement, recommendation, or favoring by the United States Government or any agency thereof. The views and opinions of authors expressed herein do not necessarily state or reflect those of the United States Government or any agency thereof.

Reactor and Nuclear Systems Division

Thermophysical Property Measurements of Salt Mixtures

N. Dianne Bull Ezell
Ryan Gallagher
Nicholas Russell
Alex Martin
Abbey McAlister
Jake McMurray

Date Published: August 2020

Prepared by
OAK RIDGE NATIONAL LABORATORY
Oak Ridge, TN 37831-6283
managed by
UT-Battelle, LLC
for the
US DEPARTMENT OF ENERGY
under contract DE-AC05-00OR22725

CONTENTS

LIST OF FIGURES	v
LIST OF TABLES	vii
ACKNOWLEDGMENTS	ix
EXECUTIVE SUMMARY	xi
1. BACKGROUND	1
2. DENSITY MEASUREMENT	2
2.1 Description of Method: Archimedes Bob	2
2.2 Explanation of Test Apparatus	2
2.3 Testing Results	3
3. SPECIFIC HEAT MEASUREMENT	5
3.1 Description of Method: Differential Scanning Calorimetry (DSC)	5
3.2 Explanation of Test Apparatus	5
3.3 Testing Results	5
4. THERMAL CONDUCTIVITY MEASUREMENT	7
4.1 Description of Method: Variable Gap	7
4.2 Explanation of Test Apparatus	7
4.3 Testing Results	8
5. VISCOSITY MEASUREMENT	11
5.1 Description of Method: Falling Ball Viscosity - Optical and X-Ray	11
5.2 Explanation of Test Apparatus	14
5.3 Calculations and Results	14
5.3.1 Theoretical Investigation of Wall Effects	15
5.3.2 Theoretical Investigation of Various Fluids	16
5.3.3 Initial Optical Testing	18
6. SUPPORTING INTERNAL AND EXTERNAL ACTIVITIES	20
7. CONCLUSIONS AND FUTURE WORK	21
8. REFERENCES	23

LIST OF FIGURES

1	Archimedes bob density measurement test apparatus	3
2	Density measurement calibration testing results using Nitrate (MS-1) salt	3
3	Schematic of the Netzsch Pegasus 404C DSC measuring head: reference crucible is shaded.	6
4	DSC specific heat testing results: FLiNaK.	6
5	Variable gap thermal conductivity assembly.	8
6	Variable gap thermal conductivity.	9
7	Variable gap thermal conductivity calibration testing result using nitrate (MS-1) salt.	10
8	Illustration of anticipated forces on falling ball while in angular set-up.	12
9	Illustration of the crucible design for the falling-ball x-ray viscosity system.	15
10	Illustration of x-ray viscometer set-up.	15
11	Wall effects on terminal velocity and Re for C-276/water system.	16
12	Terminal velocity for water/C-276 (20 °C), ethanol/C-276 (20°C), and FLiNaK/C-276 (600 °C) at $\theta = 10^\circ$	17
13	Re for water/C-276 (20°C), ethanol/C-276 (20 °C), and FLiNaK/C-276 (600°C) at $\theta = 10^\circ$	17
14	Viscosity data vs. literature results of nitrate (MS-1) salt.	18
15	Time-lapse image of bubble formation.	19

LIST OF TABLES

1	Input values for FLiNaK-Mo drag force calculations	16
---	--	----

ACKNOWLEDGMENTS

This work is funded by the US Department of Energy's Office of Nuclear Energy, Molten Salt Reactor (MSR) Campaign under the Advanced Reactor Technology (ART) program. The authors would like to thank Matt Kurley, Paul Rose, and Jordan Massengale.

EXECUTIVE SUMMARY

Thermal conductivity, specific heat, viscosity, and density are critical properties for understanding thermal hydraulics of heat transfer fluids (HTFs) like molten salts. These properties are important for design and safe operation of any HTF loop. These characterizations are required to benchmark computational chemical models that are used to predict properties, but existent data are limited. These measurements are extremely difficult to make due to the operating temperature range and corrosive properties of the salt. Density measurements are needed to predict volumetric behavior. Thermal expansion mismatches can cause mechanical failure of structural materials and important components that are in contact with the molten salt. All of these properties are related to heat transfer in HTFs. The heat generated in a reactor must be high enough to derive power; however it should not be so hot that it cannot be safely removed via the HTF at an appropriate rate. It is important to understand the thermal hydraulics required to operate at the desired power generation level and to avoid situations in which thermal shifts can damage components, cause failure of structural materials, and/or lead to accidents. Understanding these thermal properties can aid in component and process design and can contribute to optimized operational and safety parameters.

1. BACKGROUND

Thermophysical characterization of molten salts is essential for the design, analysis, and performance optimization of molten salt reactor concepts. However, these properties are notoriously difficult to measure, and there are major gaps in existing data for reactor-relevant salts. Therefore, Oak Ridge National Laboratory (ORNL) developed a suite of tools and procedures to measure the thermophysical properties of molten salts, including the Archimedes-bob density, variable-gap thermal conductivity, and x-ray falling-ball viscosity test systems. The data generated from these measurements will directly feed into the thermophysical database under development at ORNL and Argonne National Laboratory (ANL). Specific heat can be used to further develop the Molten Salt Thermodynamic Database (MSTDB) in collaboration with the University of South Carolina. Multiple national laboratories and universities will participate in a round-robin experiment performing characterizations of a single large batch of FLiNaK salt.

2. DENSITY MEASUREMENT

Density and thermal expansion are crucial fundamental properties that describe the volumetric behavior (mass per unit volume) of fluids with respect to temperature. To ensure the structural integrity of system components, structural analyses are often performed. Thermal expansion mismatches can cause mechanical failure of structural materials and important components that are in contact with the molten salt. Density and expansion are also essential factors in determining the effectiveness of heat transfer in fluids, and they are required when running computational fluid dynamics codes used in design and safety bases and are necessary for bench-marking predictive chemical modeling methods such as molecular dynamics.

2.1 Description of Method: Archimedes Bob

The Archimedes method is commonly used to measure the density of liquids at high temperatures Jin-Hui et al. [2013] and Cohen and Jones [1954]. A custom system using this technique was built and installed within a glove box at ORNL. The system uses a mass/volume calibrated high purity platinum plummet (bob) suspended from a precision balance by a thin metal wire. The bob is lowered into a crucible located inside a temperature-controlled furnace. While immersed, the balance is used to measure the weight of the immersed bob. The bob volume is calibrated using the measured weight in air and in a calibration fluid at room temperature, as well as the known density of platinum using Eq. (1):

$$V_0 = \frac{m_0 - m_1}{\rho_w} + \frac{\pi D \sigma_w}{\rho_w g}, \quad (1)$$

where V_0 is the volume of the plummet, m_0 is the weight of the platinum plummet in air, m_1 is the weight of the platinum plummet in distilled water, ρ_w is the density of water, D is the diameter of the suspension wire, σ_w is the surface tension of water, and g is the gravitational acceleration.

The density of salt can then be determined by the difference in the measured weight of the platinum plummet when submerged in air and in molten salt divided by the calibrated volume of the plummet. Using the known diameter of the wire, correction can be made for the surface tension force on the suspension wire. A correction for the plummet's thermal expansion must also be added using platinum's coefficient of thermal expansion. The density of salt is given by Eq. (2):

$$\rho_s = \frac{m_0 - (m_2 + \pi D \sigma_s / g)}{V_0 (1 + \alpha (T - 298))^3}, \quad (2)$$

where m_2 is the weight of the platinum plummet in molten salt, σ_s is the surface tension of molten salt, α is the platinum's coefficient of linear thermal expansion, and T is the molten salt temperature.

2.2 Explanation of Test Apparatus

The density system is located a glove box with a thermal well extending bellow the floor of the box, which holds a three-zone tube furnace. The outside of the well is cooled with water filled tubing that recirculates through a chilling system. This ensures that the internal temperature of the glove box is maintained within proper operating temperatures. The balance mounted on a fixture above the thermal well with the platinum

bob suspended from the bottom of the balance by a thin metal wire. The mounting fixture features a linear stage that raises and lowers the platinum bob into and out of the furnace. Inside the furnace cylindrical crucibles are used to hold the molten salt of interest near the axial midplane of the furnace, see Figure 1. Measurements are taken after lowering the platinum plummet into the crucible and waiting for the balance to stabilize. The plummet remains in the crucible when moving to higher temperatures

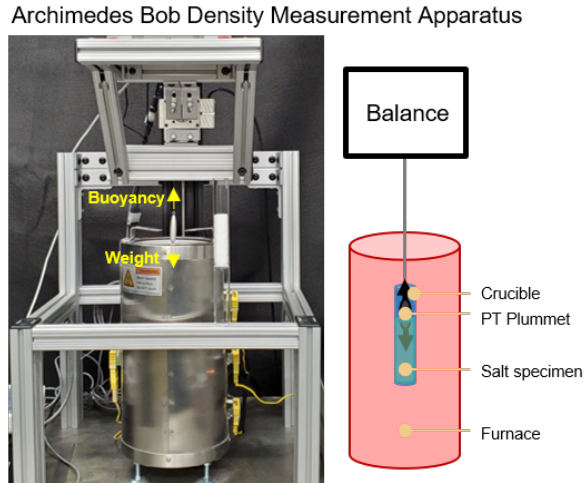


Figure 1. Archimedes bob density measurement test apparatus

2.3 Testing Results

Calibration testing was performed on the Dynalene MS-1 outside of the glove box to validate the setup and method. The results are shown in Figure 2. The maximum relative error was found to be less than 6%, with the largest deviation at low temperatures. The source of this error was likely caused by a nonuniformly melted specimen during measurement. Additionally, correction was not made for the surface tension of this salt since it is not available, and it would tend to bias measurements towards a slightly higher calculated density.

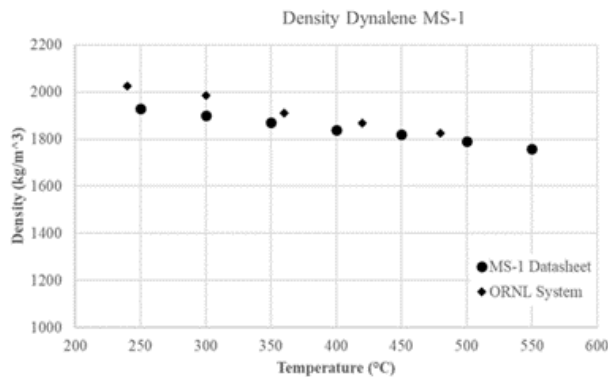


Figure 2. Density measurement calibration testing results using Nitrate (MS-1) salt

If Archimedes method were applied to fueled salts, then the major drawbacks would be the requirement for

known surface tension values, the use of an open-top crucible, and the potential for salt wetting and migrating up the wire, which could result in system contamination when using fluids with high wettability or volatility. However, under stringent preparation procedures and handling, this method could be used to measure more hazardous salts. Density measurement by dilatometry offers several advantages since it can be performed in a sealed system, and none of the instrumentation would need to contact the salt. This technique is currently under development at ORNL.

3. SPECIFIC HEAT MEASUREMENT

Specific heat relates materials mass to the amount of energy required to raise its temperature: it is the amount of heat energy stored per unit mass as a function of temperature. Specific and volumetric heat capacities are essential in understanding a fluid's ability to store and transfer heat, and furthermore, they are crucial inputs to the thermal analysis and fluid dynamics codes used to perform design and safety basis analyses.

3.1 Description of Method: Differential Scanning Calorimetry (DSC)

Heat flux differential scanning calorimetry (DSC) was used to measure the specific heat of FLiNaK. The technique uses two thermocouples that measure the temperature difference between a sample and a reference resulting from dynamic heating Boettinger et al. [2007]. The thermocouples are connected by a heat flow path of well-defined geometry and thermal properties (i.e., thermal conductivity and specific heat). This allows the differences in temperatures to be correlated to heat flow via mathematical formalisms to yield quantitative specific heat data.

The procedure calls for an empty sample crucible and an empty reference crucible to be subjected to a series of runs to establish a repeatable background. This can take three or more iterations. In this work, a temperature program was chosen that would be identical to all subsequent runs. Once the background was determined to be repeatable, the specific heat of the reference, in this case sapphire, was measured to yield calibration information. Next, the sample was placed in the same crucible that was used for the previous runs, and the final measurement was made. Each run was made with a carrier gas of ultra-high purity Ar from Airgas flowing at 100 cc/min, passed over hot Cu at 650°C to bring residual impurities such as O₂, H₂O, and other oxygen bearing vapor species to sub ppm levels. The reference crucible was never removed. The heating rate was 10°C/min from room temperature to 800°C.

3.2 Explanation of Test Apparatus

Measurements were performed on a eutectic composition of ECS FLiNaK using a Pegasus 404C DSC from Netzsch Gerätebau GmbH (Selb, Germany). This is a commercially available system that is calibrated upon delivery. Figure 3 is an illustration of the measuring head. The crucible was made of glassy carbon with a gravity sealed lid. It was separated from the Pt stage by an alumina diffusion barrier to prevent dissolution of C into the Pt, a reaction that would produce or consume heat energy and cause inaccurate results.

3.3 Testing Results

The results show good agreement with the data measured by Rogers et al. [1982] and the calculated specific heat using the MSTD Besmann et al. [2019], as can be seen in Figure 4. While glassy carbon works well for FLiNaK, other crucibles are currently under development for use with more aggressive salts, such as those with high vapor pressures and deleterious wetting characteristics.

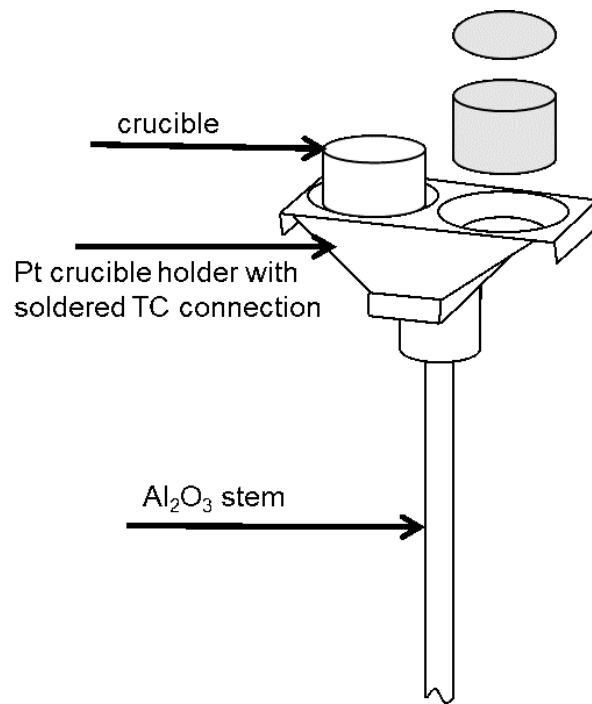


Figure 3. Schematic of the Netzsch Pegasus 404C DSC measuring head: reference crucible is shaded.

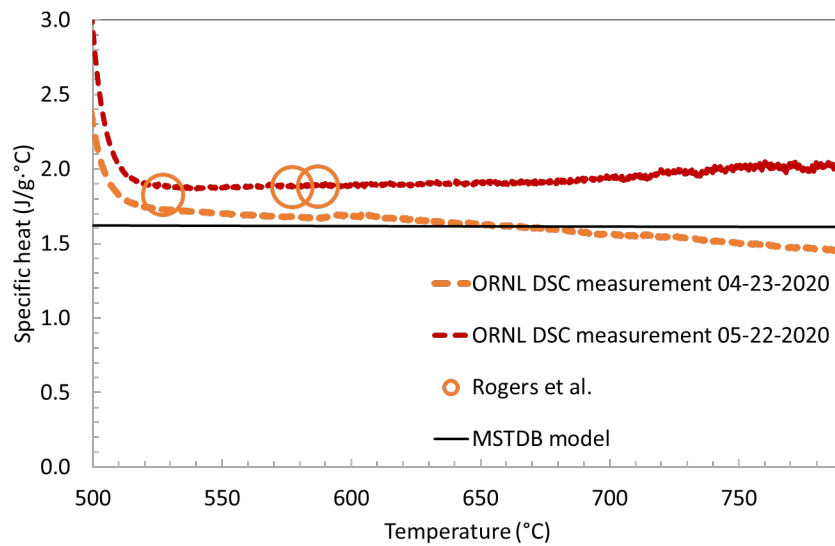


Figure 4. DSC specific heat testing results: FLiNaK.

4. THERMAL CONDUCTIVITY MEASUREMENT

An understanding of thermal conductivity is needed to understand the time-temperature dependence of heat energy flow in a material. For molten salts, data for this property—along with specific heat, viscosity, and density—is required for thermal hydraulic modeling and simulation.

4.1 Description of Method: Variable Gap

The variable gap experiment was originally designed in the 1970s at ORNL to measure the thermal conductivity of molten salts at varying temperatures. The apparatus described herein is a stainless-steel prototype that was used to validate the method and to refine the design of a C-276 variable gap experiment.

Thermal modeling and simulations were used to ensure that ORNL's design was optimized, including sizing of the gap, power supply selection, thermocouple selection, and heater designs. The test apparatus was calibrated using Ar and He to achieve the low 5% error as seen in the well-documented thermal conductivity of these gasses. The first FLiNaK salt experiments were initiated in September of 2019, only one year after the preliminary literature review. The results were promising, with high repeatability.

The system is designed to force heat to flow downward through a small sample of salt by applying heat above the salt in an inner containment element and cooling in the outer containment channels. The entire fixture is held in a temperature-controlled furnace.

4.2 Explanation of Test Apparatus

The experiment features an outer containment that is inserted into a tube-style clam-shell furnace that is used to heat the experiment. The outer containment is sealed at the bottom by being welded onto a bottom plate. A conflat flange is welded to the top of the outer containment, which is used to seal and fasten the container to the internal containment, as seen in Figures 5 and 6. Figure 6 is a mechanical drawing of the variable gap apparatus assembled inside the clam shell furnace. The furnace would be closed during operation but is drawn open here to show that the salt specimen inside the crucible is located in the center heating region (or most stable heating zone) of the furnace.

The top weldment of the internal containment is comprised of a flange that mates to the top of the outer containment, an inner tube that runs through the center of the flange, a welded stainless steel bellows, and in the middle, a conflat flange that connects to the remainder of the inner containment. The top weldment allows for the internal containment to be precisely translated axially within the outer containment while still providing a seal. The translation is controlled by a jam nut and a retaining plate located on the top conflat flange. Rotating the jam nut, which is threaded around the top portion of the inner tube, moves the entire inner containment axially.

The bottom portion of the inner containment features a tube with two welded conflat flanges on the top and bottom. The top of the tube connects to the top weldment, and the bottom connects to a heater cell. The heater cell was designed so that multiple heater designs could be used and easily replaced without have to build a new experiment. This is important since maintaining thermal uniformity across the heater is essential for reliable measurements. More optimized heaters could and should be added to future design iterations. This also allows for heaters to be included that feature more instrumentation, such as additional thermocouples, distributed temperature monitors, and flux meters.



Assembly of 2019 thermal conductivity test apparatus

Figure 5. Variable gap thermal conductivity assembly.

Another flange is located at the top of the inner tube to allow for instrumentation feedthroughs, such as a shaft-sealed quartz rod for gap measurements. Because of its low thermal expansion, the quartz rod is used to measure the variance in the gap between the heater cell and the bottom of the outer containment. A stand holding a precision variance indicator is used to measure quartz rod movement.

The component machining and welding was completed by Vacuum Technologies Incorporated (VTI), Oak Ridge, Tennessee. All parts were made from stainless steel. Stock flanges from Kurt J. Lesker, Pittsburgh, Pennsylvania, were used in the design version described here, but the mechanical drawings are detailed so that flanges can be machined from plate material. This is necessary since stock flanges made of Inconel or C-276 are typically not available off the shelf.

To assure part quality and accuracy in accordance with the drawings, inspections were independently performed at VTI by ORNL. Each part was checked with respect to the mechanical drawings. Even though this is not a requirement for this experiment, the variable gap experiment could be used for measurements in compliance with American Society for Mechanical Engineers (ASME) ASME Nuclear Quality Assurance (NQA-1) requirements. In this case, a full inspection would be required, likely by the ORNL Metrology group.

4.3 Testing Results

There are several advantages to using variable gap measurement over other thermal conductivity measurement equipment like laser flash or hot disk:

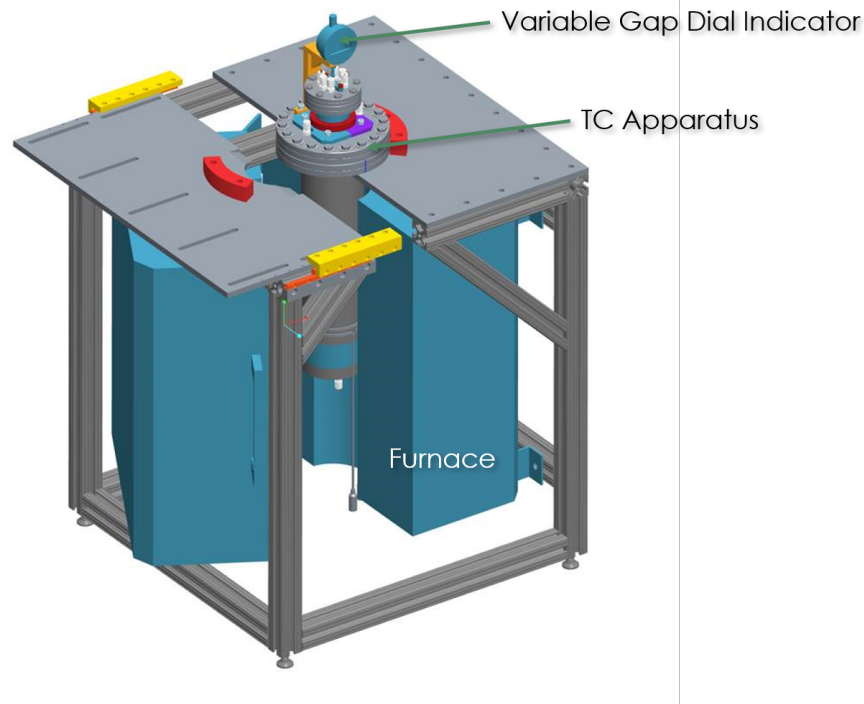


Figure 6. Variable gap thermal conductivity.

1. **Robust construction.** The variable gap system can be constructed from a wide range of alloys, allowing material compatibility to be considered when planning measurements on highly corrosive salts. The instrumentation is limited to thermocouples, which are reliable in radioactive environments and at high temperatures but do not contact the specimen. The data acquisition systems can be located away from the system if radioactive salts are present. There are minimal moving parts in the variable gap system that could fail during operation that could require maintenance; the welded bellows has shown reliability with extensive (700+ hrs) operation at elevated temperatures.
2. **Fully sealed system.** The system can be loaded and sealed in standard glove boxes, guaranteeing salt purity without the restriction of operating the entire experiment under an inert environment. The internals can be cleaned by H₂-Ar mixed gas prior to loading, with minimal changes to the setup. The system can operate at slightly elevated pressures ~25psi, which can mitigate bubble entrapment. There is little risk of contamination from volatile or radioactive salt since the system is fully sealed.
3. **Modular construction.** The components having the highest exposure to salt are replaceable and fabricated using conventional machining processes.
4. **Relatively Inexpensive.** A full system costs approximately \$25–40K, depending on the alloy. If ordered in bulk, it would be even less expensive.

The commercially available laser flash is ~\$150K+ per system and the test crucibles used inside the system are not sealed forcing the system to operate in an inert atmosphere. Furthermore, they have sensitive instrumentation and controls (I&C) making them more susceptible to uncertainty. The transient needle or

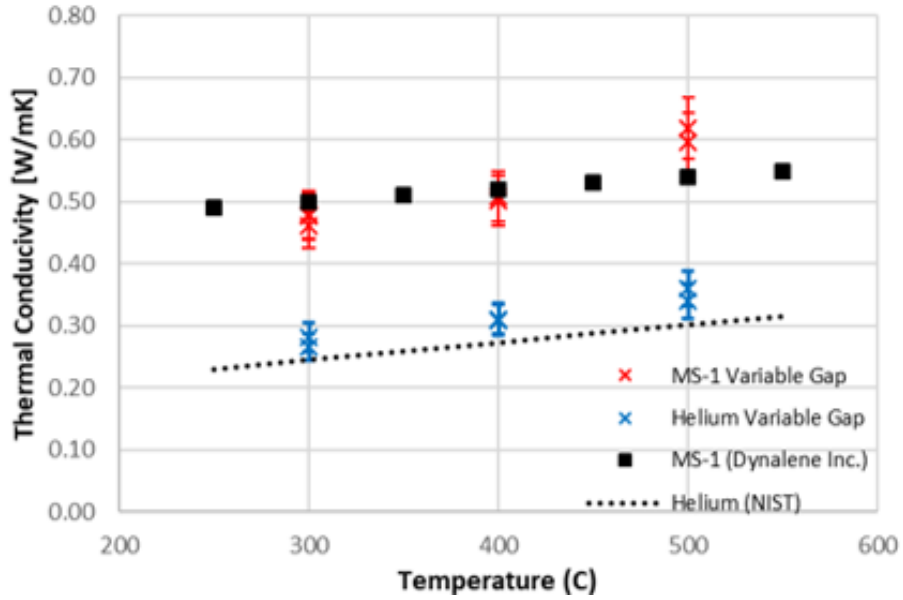


Figure 7. Variable gap thermal conductivity calibration testing result using nitrate (MS-1) salt.

disk sensors have a low technology readiness level (TRL) for high-temperature corrosive fluids. Substantial material and engineering design research is still needed to ensure that a crucible could survive molten salts and clean room fabrication. Also, coating deposition are typically required for transient needle or disk sensors driving up the overall cost of the measurement. Finally, additional research and development into coating deposition methods would be required before transient needle or disk sensors would be reliable testing options.

5. VISCOSITY MEASUREMENT

Measuring the viscosity of the molten salt is important because it is a property that is directly relevant to fluid flow and heat transfer behavior, and it is important when sizing loop components and determining pumping capacities.

5.1 Description of Method: Falling Ball Viscosity - Optical and X-Ray

Optical and x-ray viscosity measurements are based on the observation of a ball rolling through a fluid-filled capillary tube. Initially, ORNL developed an optical falling-ball viscometer for chloride salt systems. The optical measurement is a good proof-of-principle apparatus, but it quickly became apparent that it would not survive the more corrosive salts containing fluoride and other hazardous fuel salts. Therefore, an x-ray falling-ball viscometer was developed to replace the optical viscometer.

Several assumptions were made in the development of this viscometer, as detailed below.

- **Isothermal system.** It is assumed that all components of the crucible and specimen will be very close to the same temperature, so that temperature gradients across the apparatus should be negligible. This assumption is justified by using a precision, high-temperature tube furnace and ensuring a sufficient holding period for equalization prior to testing. Properly sized tube furnaces have flat temperature profiles within 1°C in the central heated zone and include fine-tuning controls.
- **Negligible friction.** Presently, there is a lack sufficient research into contact characteristics of molten salts (wetting, friction, lubrication, etc.) to accurately account for friction. Because friction is a result of contact between the ball and tube and independent of fluid, it is assumed that calibration will account for any friction effects for a specific ball-tube combination; calibration is further discussed later in this section. Moreover, the inside tube surface will be manufactured to minimize surface defects and friction forces.
- **Stokes' flow.** It will be assumed that the flow conditions within the tube are dominated by viscous forces. Viscous flows are well studied, relations are known, and the apparatus is more simply characterized. To avoid nonviscous conditions, the ball will be slowed by angling the apparatus. The flow assumption will be verified with calculations for each measurement. The angle of the apparatus will be maintained throughout the measurement.

The falling-ball viscometer measures the time required for the ball to travel or “fall” through the fluid-filled capillary tube. The dynamic viscosity of the fluid is correlated to the time required for the ball to descend a determined distance through the fluid of interest. The capillary tube’s internal diameter, the ball’s external diameter, and the window of observation length are calibrated and well known. The driving force is gravity, which can be manipulated by adjusting the inclination angle of the capillary tube. The steeper the angle of the capillary, the faster the ball will descend, leading to nonviscous conditions and invalid results, as shown in Figure 8. Assuming that there is viscous flow ($Re \ll 1$) and that the ball rolls at terminal velocity during the window of observation (verified with calculations from literature), all forces on the ball will be in equilibrium. The three forces used to determine the viscosity equation are (1) the angled portion of the gravitational driving force (F_G), (2) the opposing viscous force (f), and (3) the opposing buoyancy force (F_B). It is important to note that the lift force (F_L) results from the sphere’s contact with the tube and is equal and opposite to the normal component of the ball’s weight; the lift force is constant for a given ball-tube-angle combination and is accounted by calibration.

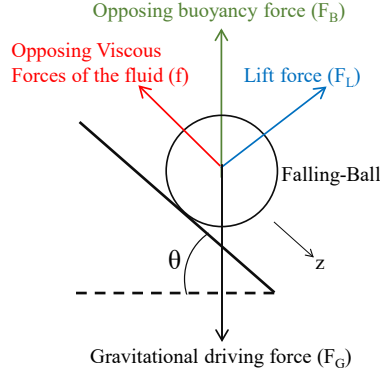


Figure 8. Illustration of anticipated forces on falling ball while in angular set-up.

Using Stokes' law, a viscous drag force is exerted on the sphere by the fluid and is directly proportional to the viscosity of the fluid (μ), the radius of the sphere (r), and the magnitude of the sphere's velocity (U) falling down the tube in the z -direction, as demonstrated in Eq. (3):

$$f = 6\pi\mu rU. \quad (3)$$

When a steel ball is dropped in a fluid-filled capillary tube and driven downward by gravity, the gravitational force is greater than the buoyant force. Therefore, the net volumetric driving force on the ball is solved using Eq. (4):

$$F_{drive} = F_G - F_B = \frac{4}{3}\pi r^3 (\rho_b - \rho_f) g \sin \theta, \quad (4)$$

where ρ_b and ρ_f are the densities of the steel ball and the fluid, respectively and F_G and F_B are defined in Figure 8.

When $F_{drive} = f$, the ball stops accelerating and falls at a constant velocity (U_t), known as *terminal velocity*, as demonstrated in Eq. (5).

$$U_t = \frac{2r^2 (\rho_b - \rho_f) g \sin \theta}{9\mu} \quad (5)$$

Based on this equation, the dynamic viscosity (μ) is calculated from the falling time (t) and distance (L), as shown in Eq. (6).

$$\mu = \frac{d^2 (\rho_b - \rho_f) g \sin \theta}{18L} t. \quad (6)$$

The capillary proportionality constant, K , is defined to simplify the equation and characterize the test apparatus. The proportionality constant absorbs constant design parameters (d , L , g , θ) and is unique to each ball-tube-angle combination. Although many attempts have been made to derive K from fluid theory

(Lewis [1953] and Hubbard and Brown [1943]), the constant can also be empirically derived using calibration with a well-known reference fluid. Calibration will also account for rolling friction and lift force effects as they are dependent only on the selection of ball, tube, and angle.

The derived Stokes' equation for viscosity is simplified in Eq. (7):

$$\mu = K \cdot (\rho_b - \rho_f) \cdot t \quad (7)$$

The Stokes' drag force is well studied and summarized in Brizard et al. [2005]. The drag force is typically calculated using a dimensionless coefficient of drag, C_d , the density of the fluid, ρ_f , the terminal velocity, U_t , and a reference area, as demonstrated in Eq. (8). It is important to note that the coefficient of drag only accounts for an object in an infinite medium (i.e., not accounting for wall effects).

$$f_\infty = \frac{1}{2} C_d \rho_f U_t^2 \pi r^2. \quad (8)$$

In a finite cylinder, the inner walls increase viscous dissipation and slow the falling ball. The correction factor, K_p , is a function of the ratio of sphere and tube diameter, d/D . Many equations computing C_d and K_p are reviewed in Oseen [1927], Proudman and Pearson [1957], Bohlin [1960], Francis [1933], Haberman and Sayre [1958], Faxen [1923].

Using this correction factor, Stokes' drag is multiplied by the correction factor to be:

$$f = 6\pi\mu r U K_p. \quad (9)$$

As there are two different drag force equations, the influence of wall effects were investigated to identify applicable correlations, as seen in the calculations section. Using the corrected drag force in Eq. 9 and a correction factor, K_p , the terminal velocity, U_t , due to wall effects is corrected:

$$U_t = \frac{2r^2 (\rho_b - \rho_f) g}{9\mu K_p} \sin \theta. \quad (10)$$

It is important at this point to state that the Reynold's number— Re in Eq. (11)—is a dimensionless quantity in fluid dynamics that is used to characterize flow patterns in different flow situations, where

$$Re = \frac{\rho v_t d}{\mu}. \quad (11)$$

The dimensionless quantity is the ratio of inertial forces to viscous forces. For rolling ball viscometry, the flow must be governed by viscous forces ($Re \ll 1$); otherwise, Stokes' Law requires corrections. The falling ball is observed either through an optical technique using a camera or using an x-ray technique. The optical technique was originally developed to measure viscosity of chloride salt systems. However, this technique requires the view port or capillary and salt to be transparent. Fluoride salts attack quartz after a short period of time and cloud the container, making it opaque and no longer transparent. For this reason, ORNL switched to an x-ray technique, which allowing the use of metal containers for fluoride salts and

more hazardous fuel salt systems. Additionally, the capillary is sealed, allowing the work to be performed outside a glove box. This document only discusses the x-ray radiography.

X-ray radiography is a potential way to measure the position of a falling ball within an opaque tube. When the capillary tube is placed between an x-ray generator and a detector array, the solid sphere will attenuate more incident x-rays than the surrounding fluid, and spatial differences in electromagnetic intensity will reach the detector array. If the intensity difference is large enough with respect to the detector's sensitivity, then the sphere position will be discernible on the radiograph. The attenuation of a beam of x-rays or gamma rays passing through a sample is described as follows:

$$I = I_0 \exp(-\mu \rho x), \quad (12)$$

where I_0 is the intensity of incident beam, I is the intensity of transmitted beam, μ is the mass absorption coefficient of sample, ρ is the density of the sample, and x is the thickness of the sample (salt). Attenuation calculations are helpful for material selection and system design; the ball's position must be discernible in the radiograph for this method to be valid. The x-ray system set-up is described in the next section; a summary of the viscometry measurement using Stokes' Law is described below:

1. Set a known distance to observe.
2. Record the ball falling through the tube (optical or x-ray) at terminal velocity.
3. Determine the time of fall.
4. Calculate the viscosity (μ) using Eq. (7) and the calibrated constant K .

5.2 Explanation of Test Apparatus

A crucible (Figure 9) containing a quantified volume of salt is placed inside a furnace. The crucible is designed to have a measurement window containing the salt (the smaller diameter cylinder) and a loading section (larger cylinder) where the ball resides. The furnace is fixed to the desired angle for the viscosity measurement and is powered to the first temperature measurement point. Once the salt is molten, the crucible is rotated, allowing the ball to fall into the measurement section of the crucible.

The x-ray generator and detector plate are set-up at a predetermined distance from the furnace containing the test crucible, see Figure 10. This distance is critical to generate a clear image on the detector plate. Multiple images are taken as the ball falls through the salt, however a single snapshot is shown in Figure 10. In this snapshot, the furnace coils, crucible walls and falling ball are clearly imaged using the existing set-up.

5.3 Calculations and Results

Several design parameters (d , D , L , θ , etc.) rely heavily on (1) the wall effects on drag, (2) the time and distance to reach terminal velocity, and (3) the Reynold's number. Established correlations from literature were applied for design calculations.

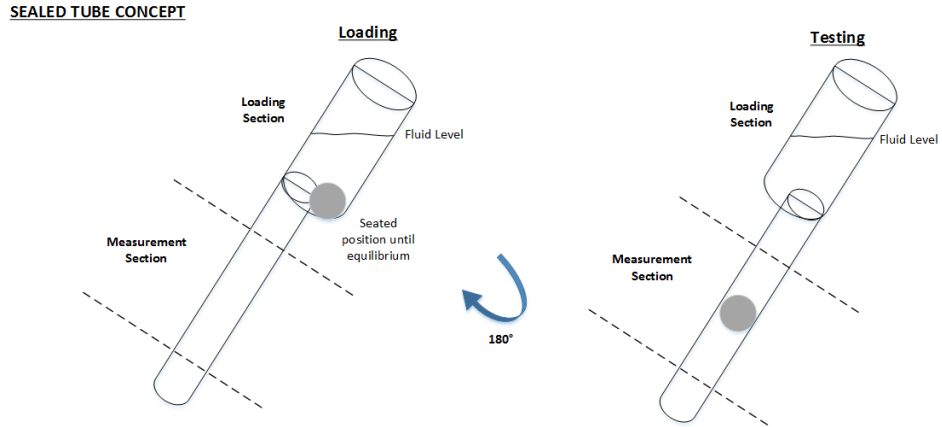


Figure 9. Illustration of the crucible design for the falling-ball x-ray viscosity system.

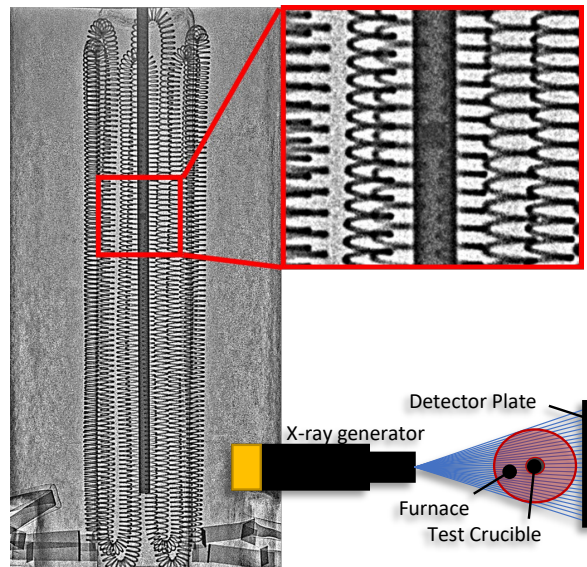


Figure 10. Illustration of x-ray viscometer set-up.

Water, ethanol, and FLiNaK were selected as theoretical fluids because of their relevance and ease of laboratory access. Kaye and Laby [1995] was used for the density and viscosity of water and ethanol. Sohal et al. [2013] was used for the density and viscosity of FLiNaK.

5.3.1 Theoretical Investigation of Wall Effects

The initial calculations used a Hastelloy C-276 ball and water as the fluid under investigation. First, the wall effects on terminal velocity were investigated for a C-276/water system at 20°C. Due to the low viscosity of water, 10° was used for the angle of inclination. Equations from the literature [Oseen [1927], Proudman and Pearson [1957], Bohlin [1960], Francis [1933], Haberman and Sayre [1958], Faxen [1923]] were used for the wall correction factor and velocity calculations. The input property values are given in

Table 1. The results from these calculations are shown in Figure 11.

Table 1. Input values for FLiNaK-Mo drag force calculations

Description	Symbol	Value	Units
Density of C-276 sphere	ρ_b	8.89	g/cm^3
Density of water at 20 °C	ρ_f	0.9982	g/cm^3
Viscosity of water at 20 °C	μ	1.0005	mPa s
Gravitational constant	g	981	cm/s^2
Inclination angle of horizon	θ	10°	degree
Tube inner diameter	D	0.8	mm
Sphere diameter	d	0.25, 0.30, 0.35, 0.40, 0.50, 0.60	mm

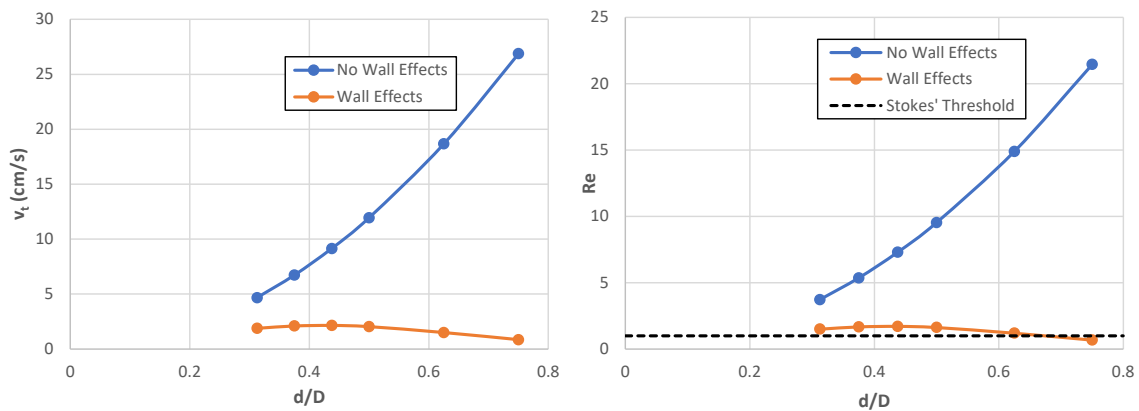


Figure 11. Wall effects on terminal velocity and Re for C-276/water system.

An inflection point is observed when wall effects are considered, which is likely caused by the eventual dominance of viscous forces (walls) over the inertial forces (increased ball size). Moreover, a ball-to-tube ratio (d/D) of 0.72 and greater results in Stokes' flow. Wall effects were determined to be significant for calculations.

5.3.2 Theoretical Investigation of Various Fluids

Next, the terminal velocity and Re calculations were repeated with ethanol and FLiNaK, accounting for wall effects. Ethanol and FLiNaK were chosen due to their availability and well-studied properties. Ethanol at 20°C has a kinematic viscosity of 0.9982 cP and a density of 0.784 g/cm^3 , per Kaye and Laby [1995]. FLiNaK at 600°C has a kinematic viscosity of 8 cP and a density of 2.05 g/cm^3 , per Sohal et al. [2013]. The angle of inclination was 10°. The results from these calculations are shown in Figures 12 and 13.

As seen from preliminary calculations for water, ethanol, and FLiNaK, the rheological properties significantly impact the flow conditions. Stokes' regime is more easily achieved at higher fluid viscosities. The viscosity of other fluoride and chloride salts is expected to be between the values for water and FLiNaK, (1–2 cP). The density of the falling sphere directly influences the inertial energy of the system.

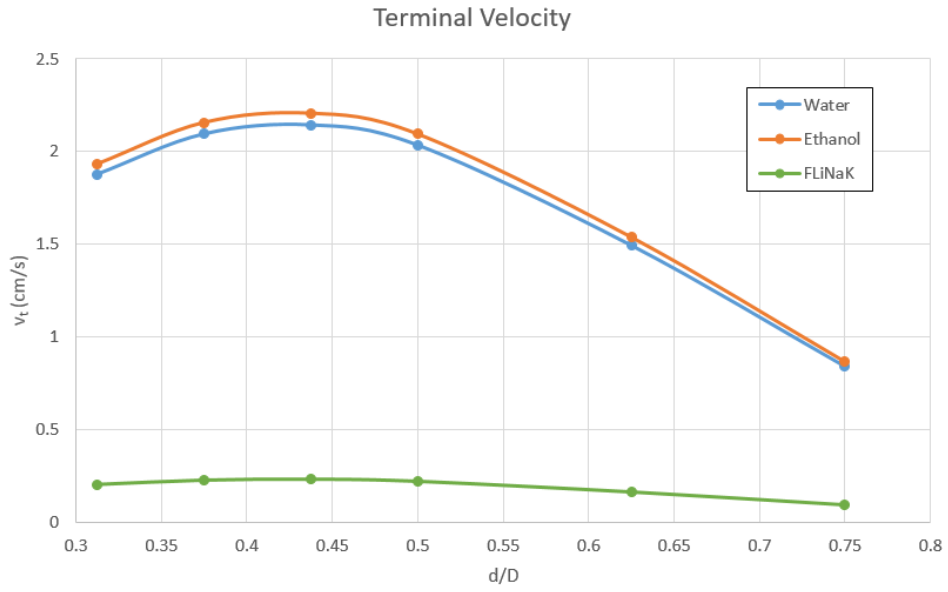


Figure 12. Terminal velocity for water/C-276 (20 °C), ethanol/C-276 (20°C), and FLiNaK/C-276 (600 °C) at $\theta = 10^\circ$.

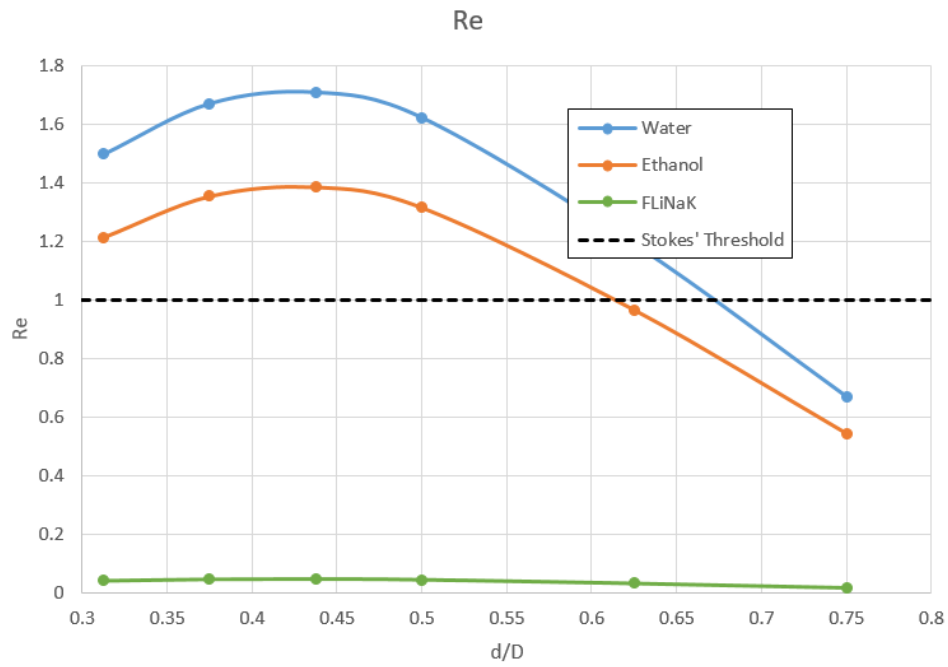


Figure 13. Re for water/C-276 (20°C), ethanol/C-276 (20 °C), and FLiNaK/C-276 (600°C) at $\theta = 10^\circ$.

The more dense the sphere, the faster the terminal velocity; the system diverges from Stokes' regime. The calculations support the feasibility of viscosity measurements using standard size tubes and spheres.

The preliminary calculations agree with accepted theory and expectations. Both terminal velocity—and

consequently flow conditions—are heavily influenced by sphere size, angle of inclination, fluid viscosity, and component densities. These results are consistent with all systems studied. Initial testing should use spheres of moderate size, ranging from 5.0–8.0 mm in diameter, and a ball-to-tube size ratio of >0.75 for smaller angles ($\theta < 10^\circ$) and >0.9 for larger angles ($10^\circ < \theta < 30^\circ$). The terminal velocity decreases at shallower angles, approaching zero at horizontal conditions. For less viscous fluids such as water or ethanol, a smaller angle of inclination is required to ensure Stokes' regime.

5.3.3 Initial Optical Testing

Initial testing employed a quartz tube ($D = 8.00\text{cm}$) and a 304 stainless steel ball ($d = 7.14\text{cm}$) to achieve a diameter ratio of 0.893. Possible reference fluids were investigated for room-temperature calibrations; water, ethanol, and heat transfer fluid "Dowtherm A" were selected for calibration. For initial testing at elevated temperatures, Dynalene MS-1, a nitrate salt, was selected due to its availability, well-known properties, and minimal hazards. The MS-1 salt was tested at temperatures ranging from 275°C to 400°C .

During testing, it became obvious that bubbles within the sample have a significant impact on the measurement, as seen in Figure 14. (Technical data from Dynalene, Inc.) Figure 15 shows a time-lapse image of the bubble formation. The cleaning, baking, and loading processes were refined to prevent bubbles in the experiment. The materials are cleaned in an ultrasonic bath, and the salt is loaded into a glove box, baked in a dry vacuum oven overnight, and then back-filled with argon. The effect of the bubbles was noticed during the optical measurements and was undetected in the x-ray system. To ensure that this does not occur in the x-ray system, the steps developed for the optical measurement must be followed.

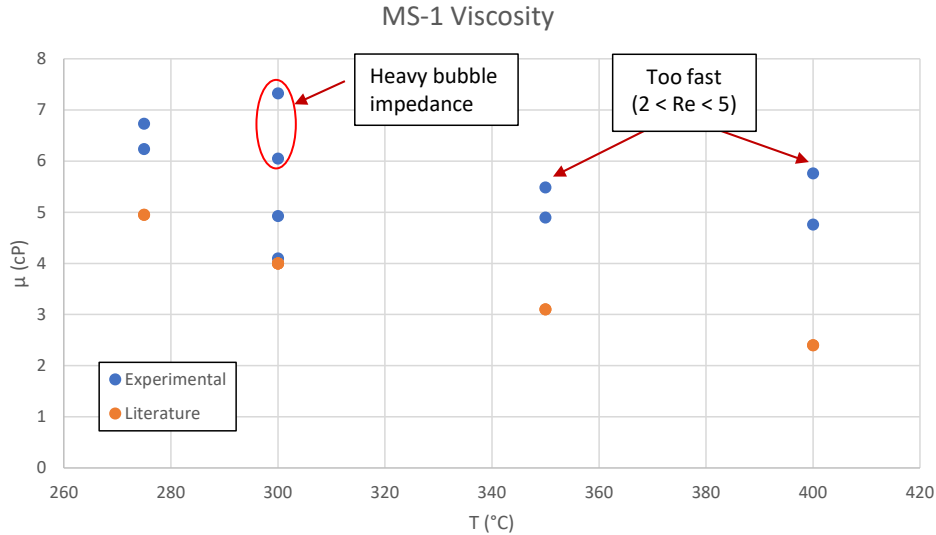


Figure 14. Viscosity data vs. literature results of nitrate (MS-1) salt.

The following tasks were completed this FY with continuing development underway:

1. Calibration procedure has been revised, resulting in precise, reliable calibration measurements.
2. Modified loading procedure was proven to reduce bubbles and error.

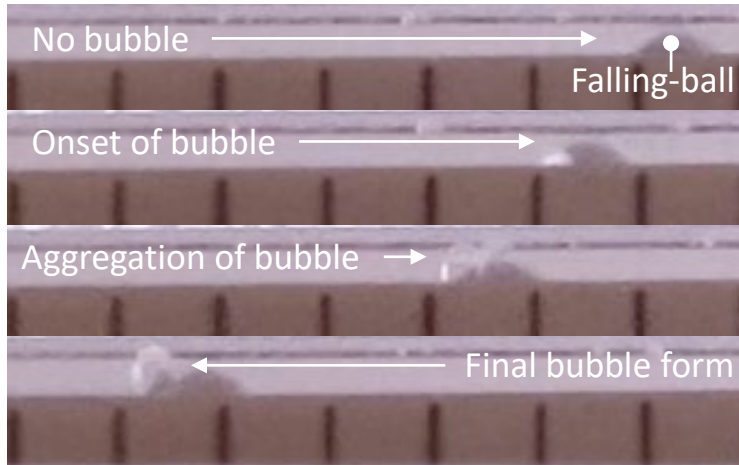


Figure 15. Time-lapse image of bubble formation.

3. Testing conditions are continuously improved through loading and design modifications.
4. Design parameters have been refined by using standard sizes.
5. Future work is planned for x-ray and refined optical measurements.

6. SUPPORTING INTERNAL AND EXTERNAL ACTIVITIES

To complete the goals scoped within this work package, many hours were dedicated to building collaborations with a diverse group of entities. At ORNL, a laboratory space was installed to support the four thermophysical measurements including a glove box for handling salts. Both coolant and fuel salts can be handled and characterized in the laboratory space. To support crucible design for the specific heat measurement, a contact angle set-up was designed and implemented for preliminary testing. Multiple publications were developed describing the systems and data, and an invention disclosure was filed listing four ORNL researchers.

ORNL collaborated with the University of Virginia and the Joint Research Centre (JRC) in the European Commission to win an International Nuclear Energy Research Initiative (I-NERI) for development of molten salt thermophysical characterizations. This collaboration will continue to build the relationship throughout national laboratories, universities, and the international nuclear community. ORNL also participated in the molten salt thermophysical property working group led by Ted Besmann at the University of South Carolina. This working group is collaborating to build a database of measured salt characterizations across a wide range of systems. ORNL recently collaborated with Idaho National Laboratory's National Reactor Innovation Center (NRIC) to help them develop their thermophysical characterization needs within their hot cell facilities. Furthermore, ORNL and Argonne National Laboratory participate in a bi-weekly meeting to continue their collaborative efforts, describe the progress made at each facility, and target areas for growth and development.

Most significantly, three characterization systems were deployed in new laboratories in less than a year for this effort. This rapid prototyping was made possible by the multidisciplinary team funded through the DOE MSR national campaign.

7. CONCLUSIONS AND FUTURE WORK

Characterization of the thermophysical properties of molten salt is critical for reactor designers in many aspects. ORNL has developed a suite of equipment to measure density, heat capacity, thermal conductivity, and viscosity. Each of these test apparatuses was designed and built to conduct preliminary characterizations. Density is measured using Archimedes' bob, heat capacity is measured using a commercially available DSC, thermal conductivity is measured using a variable gap method, and viscosity is measured using an x-ray falling-ball technique. All four systems have been calibrated using a nitrate salt (Dynaline MS-1) and are ready for the round-robin FLiNaK salt measurement. Density and heat capacity have already completed the FLiNaK measurements, and the data are available for the database.

After viscosity and thermal conductivity measurements on the FLiNaK salts are completed for the database, ORNL intends to certify the measurement test apparatuses. This would enable the generation of NQA-1 certified data for reactor developers. All the apparatuses were designed to enable a multi-salt facility (chloride and fluoride salts, coolant and fuel salts), but some modifications would be required to ensure the ability to use the systems inside a hot cell with manipulators.

8. REFERENCES

References

- Theodore M. Besmann, Johnathan Ard, Stephen Utlak, Jake W. McMurray, and Robert Alexander Lefebvre. Status of the Salt Thermochemical Database. Technical report, Oak Ridge National Laboratory, Oak Ridge, Tennessee (United States), 2019.
- William J. Boettinger, Ursula R. Kattner, Kil-Won Moon, and John H. Perepezko. DTA and Heat-Flux DSC Measurements of Alloy Melting and Freezing. In *Methods for Phase Diagram Determination*, pages 151–221. Elsevier, 2007.
- Torsten Bohlin. *On the Drag on a Rigid Sphere Moving in a Viscous Liquid inside a Cylindrical Tube*, volume 155. Elander Stockholm, Sweden, 1960.
- Matthieu Brizard, Mohamed Megharfi, E. Mahe, and C. Verdier. Design of a High Precision Falling-Ball Viscometer. *Review of Scientific Instruments*, 76(2):025109, 2005.
- S. I. Cohen and T. N. Jones. A Summary of Density Measurements on Molten Fluoride Mixtures and a Correlation for Predicting Densities of Fluoride Mixtures. Technical report, Oak Ridge National Laboratory, Oak Ridge, Tennessee, 1954.
- Hilding Faxen. Die Bewegung einer starren Kugel langs der Achse eines mit zäher Flüssigkeit gefüllten Rohres. *Arkiv for Matematik Astronomi och Fysik*, 17:1–28, 1923.
- Alfred W. Francis. Wall Effect in Falling Ball Method for Viscosity. *Physics*, 4(11):403–406, 1933.
- William L. Haberman and Rose M. Sayre. Motion of Rigid and Fluid Spheres in Stationary and Moving Liquids inside Cylindrical Tubes. Technical report, David Taylor Model Basin, Washington, DC, 1958.
- Robert M. Hubbard and George Granger Brown. The Rolling Ball Viscometer. *Industrial and Engineering Chemistry, Analytical Edition*, 15(3):212–218, 1943.
- Cheng Jin-Hui, Zhang Peng, An Xue-Hui, Wang Kun, Zuo Yong, Yan Heng-Wei, and Li Zhong. A Device for Measuring the Density and Liquidus Temperature of Molten Fluorides for Heat Transfer and Storage. *Chinese Physics Letters*, 30(12):126501, 2013.
- G.W.C. Kaye and T.H. Laby. *Tables of Physical and Chemical Constants (Kaye and Laby)*. National Physical Laboratory (Great Britain), Middlesex, England, 16 edition, 1995.
- H.W. Lewis. Calibration of the Rolling Ball Viscometer. *Analytical Chemistry*, 25(3):507–508, 1953.
- Carl Wilhelm Oseen. Neuere Methoden und Ergebnisse in der Hydrodynamik. *Leipzig: Akademische Verlagsgesellschaft mb H.*, 1927.
- Ian Proudman and J. R. A. Pearson. Expansions at Small Reynolds Numbers for the Flow Past a Sphere and a Circular Cylinder. *Journal of Fluid Mechanics*, 2(3):237–262, 1957.
- Derek J. Rogers, Toshinobu Yoko, and George J. Janz. Fusion Properties and Heat Capacities of the Eutectic Lithium Fluoride-Sodium Fluoride-Potassium Fluoride Melt. *Journal of Chemical and Engineering Data*, 27(3):366–367, 1982.

Manohar S. Sohal, Matthias A. Ebner, Piyush Sabharwall, and Phil Sharpe. Engineering Database of Liquid Salt Thermophysical and Thermochemical Properties. Technical report, Idaho National Laboratory, Idaho Falls, Idaho (United States), 2013.